



# Multivariate Phase Covariance Analysis: A new approach to revealing functional connectivity in EEG time-series



Kyle J. Curham, John J. B. Allen  
Department of Psychology - University of Arizona - Tucson, Arizona

## Introduction

Phase-synchronization is a potential mechanism to dynamically modulate functional connectivity between brain regions.

- Inter-channel Phase Synchrony (ICPS), a bivariate measure of phase-synchronization, has been used to reveal functional relationships.
- However, ICPS has several limitations:
  - Spurious correlations due to the third-variable problem.
  - Low statistical power due to multiple comparisons.

The current study overcomes these limitations with a new multivariate phase covariance analysis (MPCA) approach to infer network connectivity and mean phase differences between electrodes in EEG time-series. To validate the new method, we:

- Examine theta phase connectivity following correct and incorrect responses on a Flanker task, concomitant with the Error-Related Negativity (ERN).
- Implement an omnibus test to reveal statistically significant differences in coupling parameters between conditions.

## Model

The network state-space can be represented by a N-dimensional cube (Fig. 1).

- Each dimension varies from 0 to  $2\pi$ , corresponding to the periodic state-space for each oscillator.

Connectivity matrix	Graph	Topology
$\begin{bmatrix} 1 & \kappa_{ab}e^{i\mu_{ab}} \\ \kappa_{ab}e^{-i\mu_{ab}} & 1 \end{bmatrix}$		
$\begin{bmatrix} 1 & \kappa_{ab}e^{i\mu_{ab}} & \kappa_{ac}e^{i\mu_{ac}} \\ \kappa_{ab}e^{-i\mu_{ab}} & 1 & \kappa_{bc}e^{i\mu_{bc}} \\ \kappa_{ac}e^{-i\mu_{ac}} & \kappa_{bc}e^{-i\mu_{bc}} & 1 \end{bmatrix}$		

Figure 1: Relationship between network connectivity, graph, and topology.

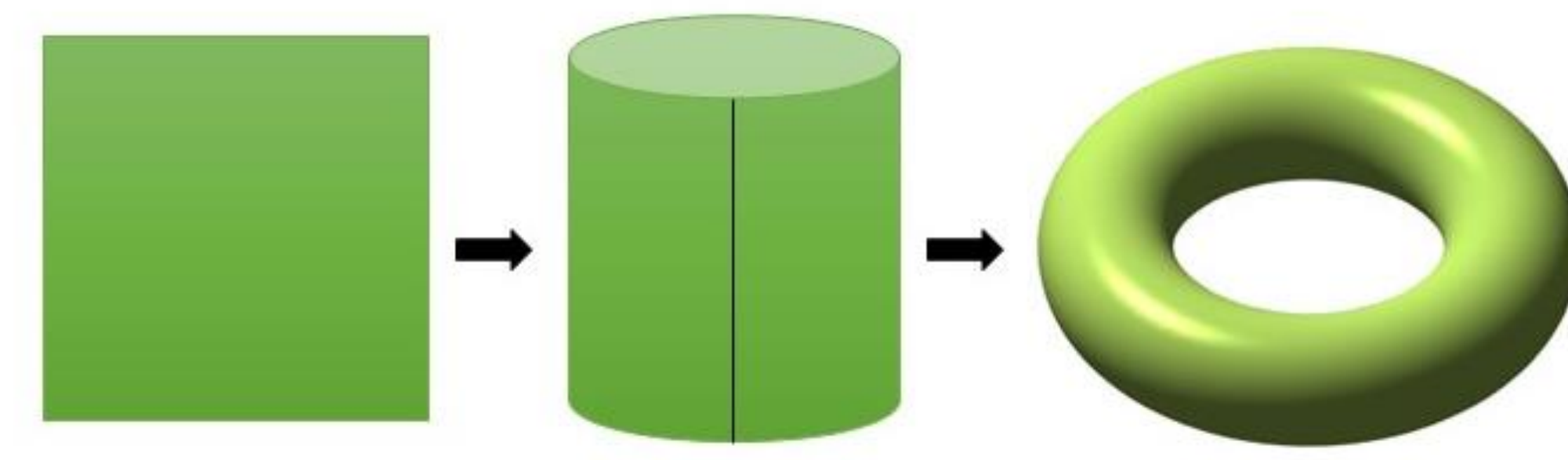


Figure 2: Example topology for a two-node network.

- Trajectories are restricted to the surface of an N-torus (Fig. 2)<sup>1</sup>.
- Attractor states of the network are described by a Hermitian-symmetric positive-definite (SPD) covariance matrix.

Minimizing the network energy (U) maximizes the log-posterior of the model:

$$U(\theta) = \frac{1}{2} X^T K X = \frac{1}{2} \sum_{i,j=1}^N \kappa_{ij} e^{i(\theta_i - \theta_j - \mu_{ij})}$$

- Where the elements of X indicate the phase of each oscillator and K is the SPD connectivity matrix.
- Gradient descent on the network energy generates trajectories in the state-space (Fig.3).

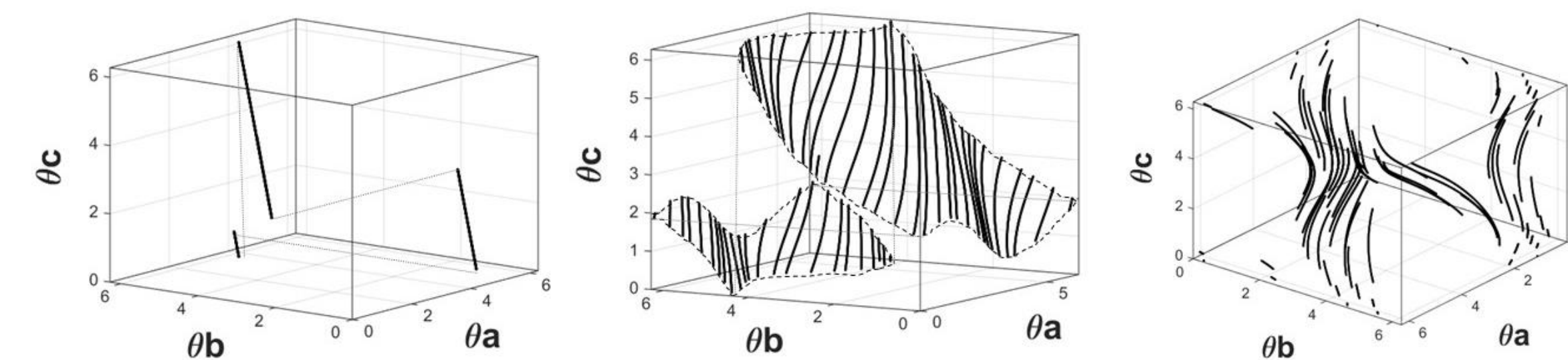


Figure 3: Example trajectories in a three-node network with varying coupling parameters.

## Model Inference

Sample covariance matrices are obtained for repeated trials over 60 EEG scalp electrodes by computing the outer product of the channel by time-point data matrix of complex-valued phases (obtained by wavelet transformation).

- The arithmetic mean of these matrices over time-points is equivalent to the mean ICPS for each pairwise combination of oscillators.
- Sample covariance matrices lie in the parameter space of the model, which is given by the manifold of symmetric positive-definite matrices (Fig. 4).
- The geometric mean is the center of mass of the points in the model parameter space.

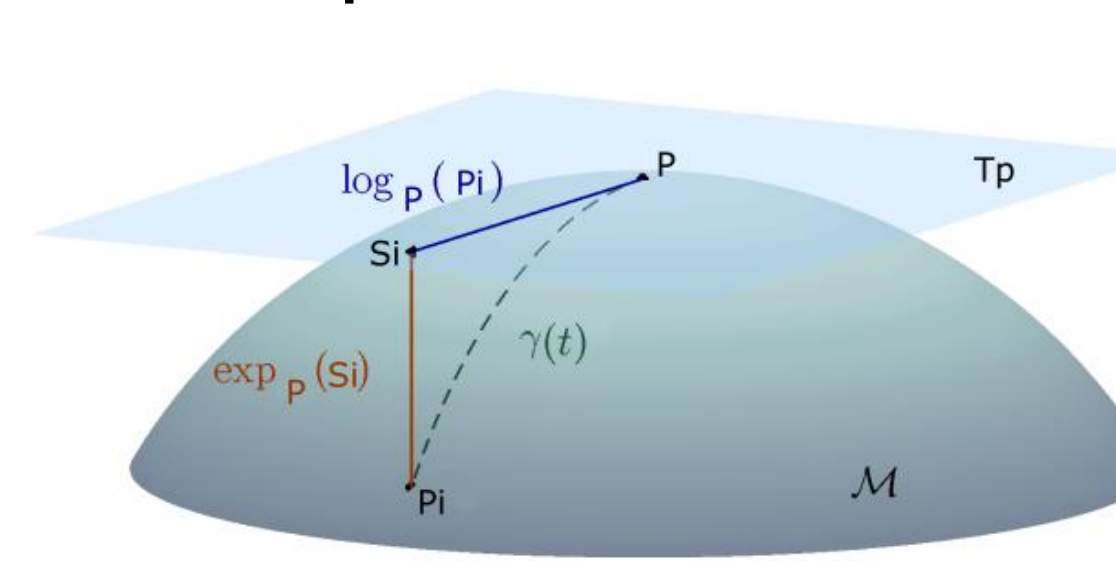


Figure 4: Parameter space for Hermitian SPD covariance matrices. Geodesics are minimal curves between points in the manifold.

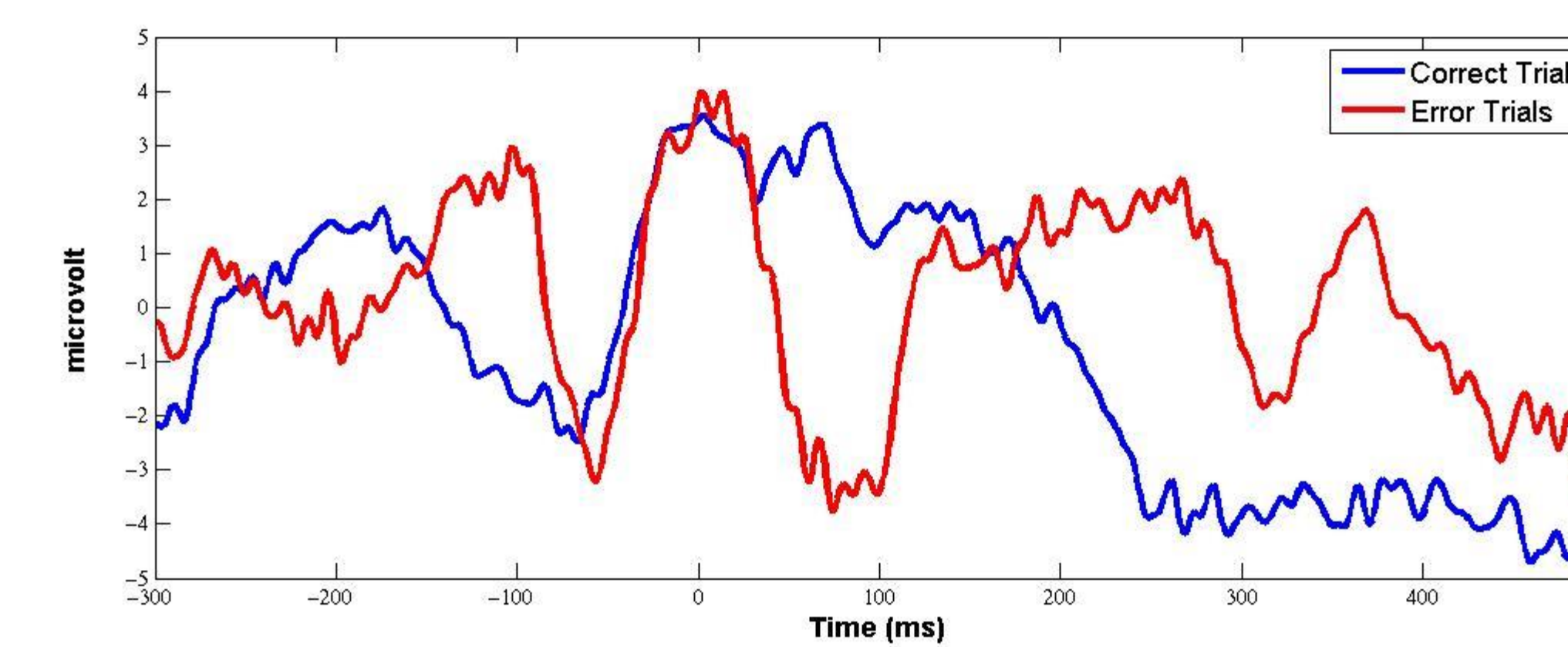
An iterative algorithm is employed on the SPD manifold to compute the geometric mean of a set of positive-definite covariance matrices.

- Minimizes the sum of squared residuals, given by the lengths of the geodesics between the group means and each labeled sample.

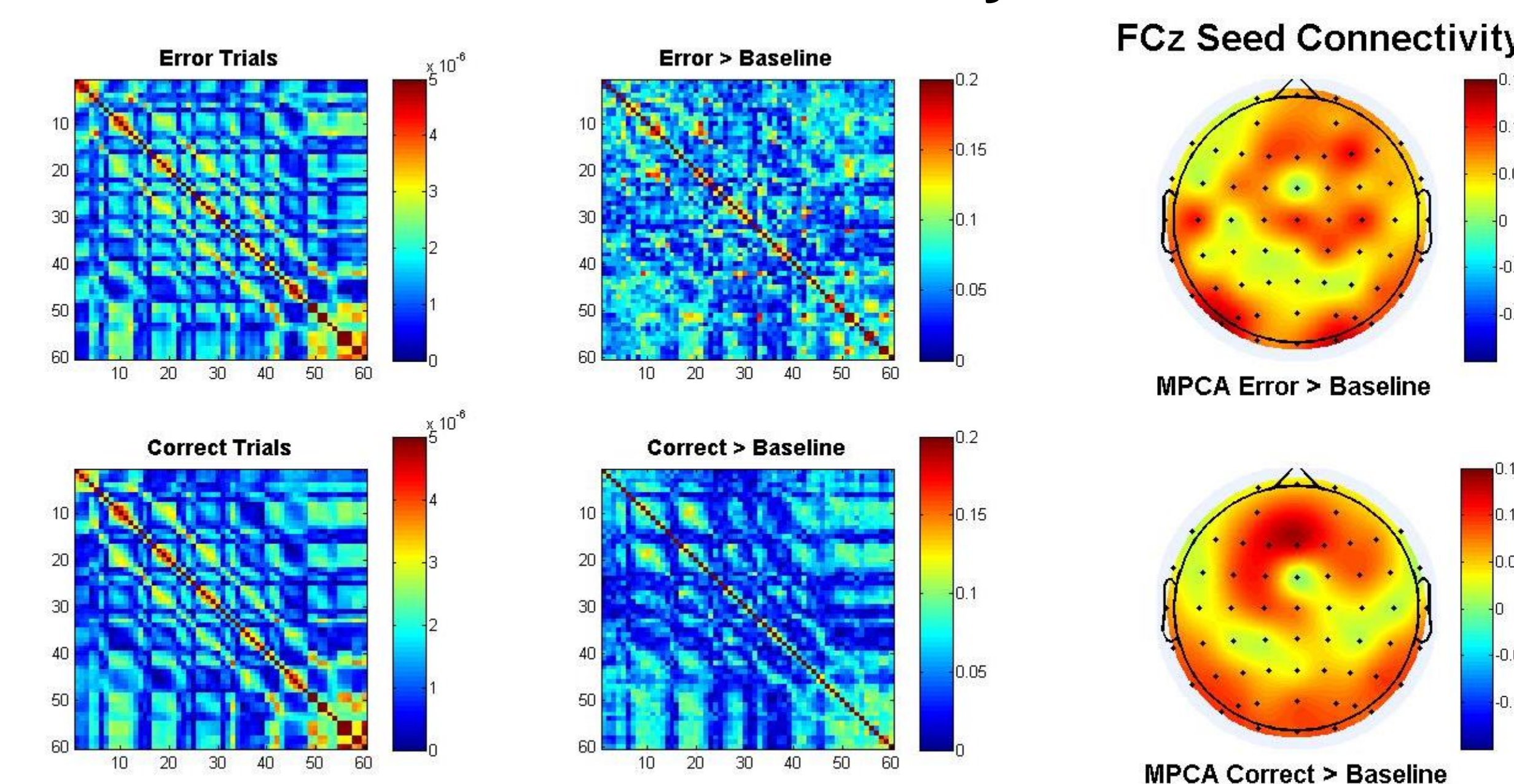
- A diffeomorphism exists between the geodesic connecting two points on the manifold, and a vector in the tangent bundle at p (Fig. 4).
- Residuals are projected into the tangent space at the current estimate and averaged to obtain a mean tangent vector.
- The point p and the mean tangent vector specify an update, with guaranteed convergence within the domain of the diffeomorphism<sup>3</sup>.

## Results

### FCz Mean ERN



### Functional Connectivity – MPCA



### Functional Connectivity – ICPS

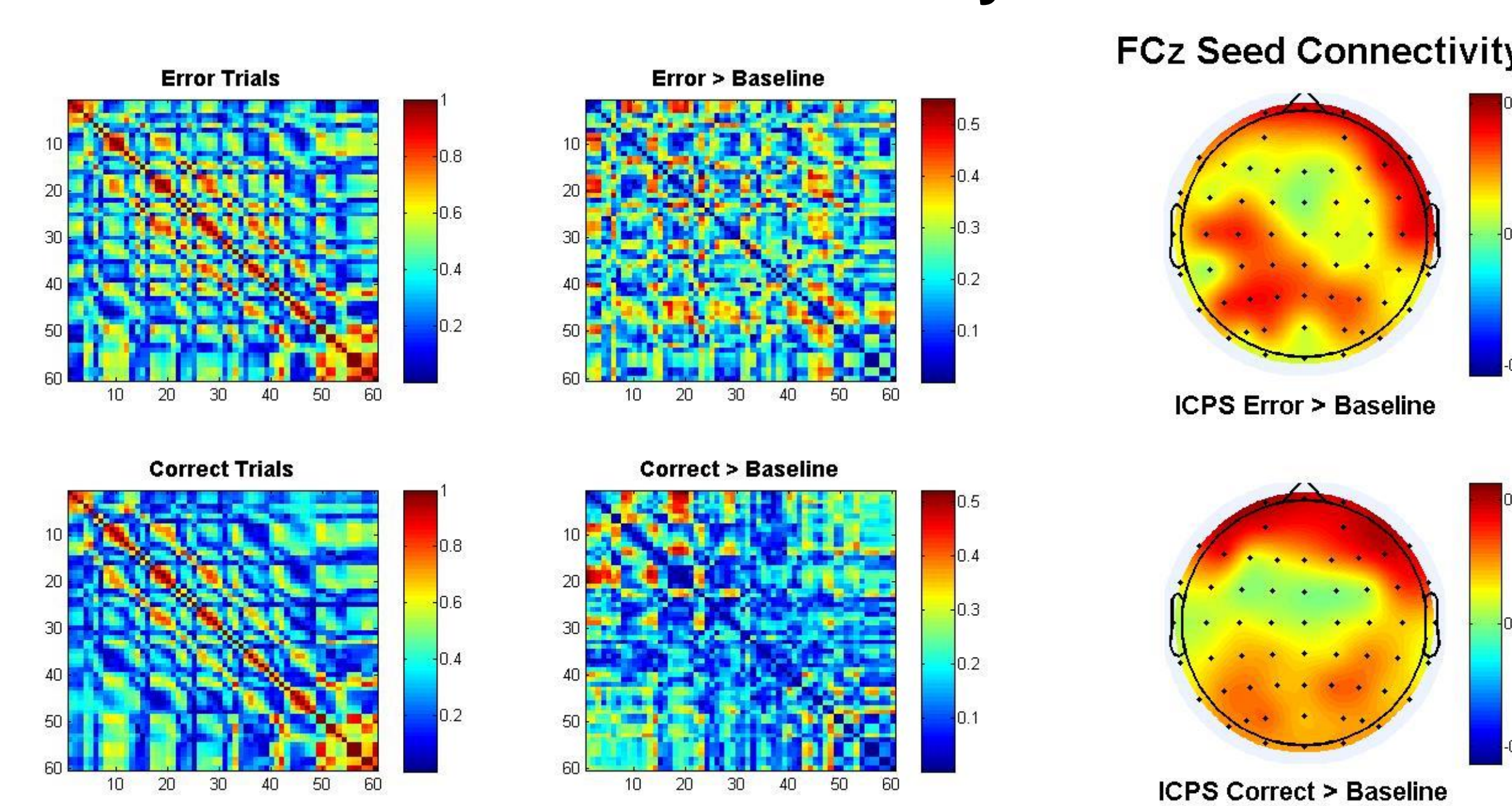


Figure 5: Functional connectivity in a single subject. (Top) MPCA was used to compute the mean connectivity for Error and Correct trials [50, -150] ms following a response, relative to the baseline period [-300, -200] ms. (Bottom) Mean ICPS was computed for comparison. Baseline corrected ICPS shows spurious results, as expected.

Significance testing between conditions is accomplished by geodesic regression with permutation testing (Fig. 6).

- Two parameter model: initial point on the manifold (one of the group means), and a tangent vector specifying the geodesic between the group means.
- Null hypothesis: the distance between the group means for is not significantly greater than zero.

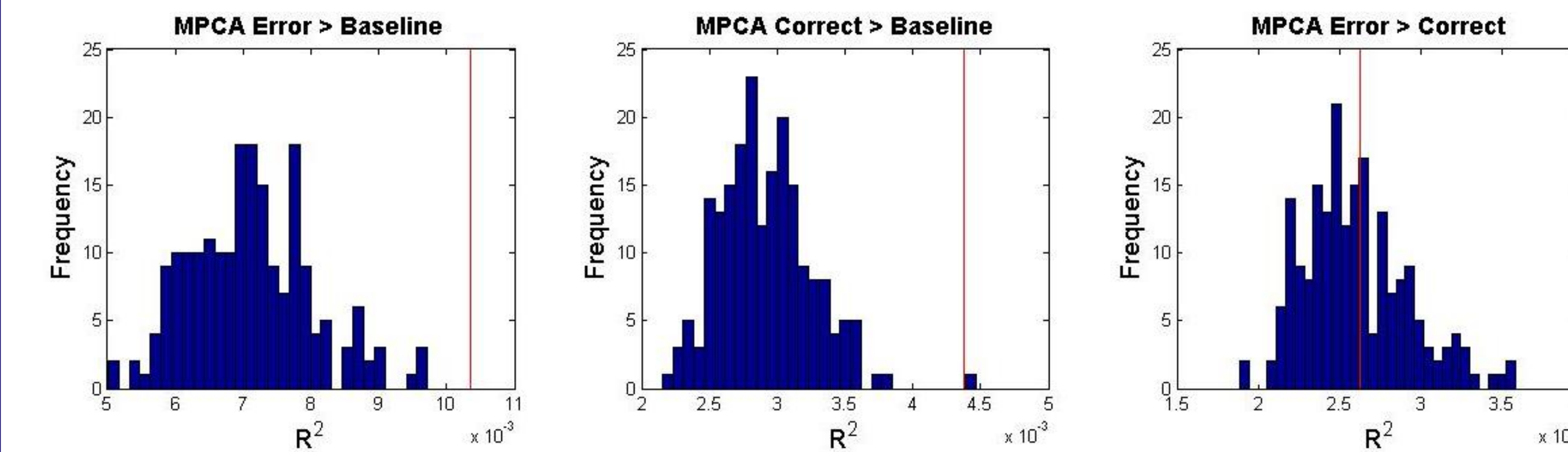


Figure 6: Expected  $R^2$  under the null hypothesis. The distribution of  $R^2$  is obtained by shuffling the data with respect to the condition labels. Error > Baseline,  $z = 3.611$ ,  $p < 0.001$ . Correct > Baseline  $z = 4.331$ ,  $p < 0.001$ . Error > Correct, ns,  $z=0.106$ ,  $p = 0.46$

## Conclusions

- Simply subtracting baseline functional connectivity matrices produces spurious results.
- Baseline-corrected MPCA provides a meaningful representation of the difference between conditions. Connectivity following error and correct trials resulted in increased connectivity relative to baseline.
- However, baseline-corrected connectivity did not differ between correct and incorrect responses.

## Future work

- Implement a geodesic regression analysis for a curve parameterized by time.
- How does the modulation in functional connectivity vary over time?
- Implement a multi-level model to analyze the difference between error and correct trials within and between participants over time.

## References

1. Cadieu, C. F., & Koepsell, K. (2010). Phase coupling estimation from multivariate phase statistics. *Neural computation*, 22(12), 3107-3126.
2. Barachant, A., Bonnet, S., Congedo, M., & Jutten, C. (2012). Multiclass brain-computer interface classification by Riemannian geometry. *Biomedical Engineering, IEEE Transactions on*, 59(4), 920-928.
3. Pennec, X., Fillard, P., & Ayache, N. (2006). A Riemannian framework for tensor computing. *International Journal of Computer Vision*, 66(1), 41-66.